



Research article

Correlation analysis and predictive model construction of metabolic syndrome, complete blood count-derived inflammatory markers, and overall burden of cerebral small vessel disease

Yang Wang^{a,b}, Yang Li^a, Shusheng Jiao^b, Yuanhang Pan^a, Xiwei Deng^b, Yunlong Qin^b, Di Zhao^a, Zhirong Liu^{a,*}^a Department of Neurology, Xijing Hospital, Fourth Military Medical University, Xi'an, China^b Department of Neurology, Bethune International Peace Hospital, Shijiazhuang, China

ARTICLE INFO

Keywords:

Cerebral small vessel disease
Neuroimaging burden
Metabolic syndrome
Complete blood count-derived inflammatory markers
Machine learning

ABSTRACT

Background: The high burden of cerebral small vessel disease (CSVD) on neuroimaging is a significant risk factor for stroke, cognitive dysfunction, and emotional disorders. Currently, there is a lack of studies investigating the correlation between metabolic syndrome (MetS), complete blood count-derived inflammatory markers, and total CSVD burden. This study aims to evaluate the total CSVD imaging load using machine learning (ML) algorithms and to explore further the relationship between MetS, complete blood count-derived inflammatory markers, and CSVD load. **Methods:** We included CSVD patients from Xijing Hospital (2012–2022). Univariate and lasso regression analyses identified variables linked to CSVD neuroimaging burden. Six ML models predicted CSVD burden based on MetS and inflammatory markers. Model performance was evaluated using ROCauc, PRauc, DCA, and calibration curves. The SHAP method validated model interpretability. The best-performing model was selected to develop a web-based calculator using the Shiny package.

Results: The Logistic regression model outperformed others in predicting CSVD burden. The model incorporated MetS, neutrophil-to-lymphocyte ratio (NLR), homocysteine (Hcy), age, smoking status, cystatin C (CysC), uric acid (UA), and prognostic nutritional index (PNI).

Conclusion: MetS, NLR, Hcy and CSVD high load were positively correlated, and the Logistic regression model could accurately predict the total CSVD load degree.

1. Introduction

Cerebral small vessel disease (CSVD) is a clinical syndrome characterized by cognitive, imaging, and pathological changes resulting from alterations in the structure and function of small blood vessels, including arterioles, venules, and capillaries [1]. With the global population aging, CSVD has become one of the most prevalent pathological processes encountered by neurologists [2]. Epidemiological studies have revealed that over 700 million individuals worldwide are affected by various forms of CSVD [3]. Moreover, CSVD is a leading cause of several neurological disorders, including 25 % of ischemic strokes, 80 % of hemorrhagic strokes, and 45 % of

* Corresponding author. 169 Changle West Road, Xincheng District, Xi'an City, Shaanxi Province, China.

E-mail addresses: a54515451@qq.com (Y. Wang), 18391696287@163.com (Y. Li), xiaojiao5678@sina.com (S. Jiao), 569369622@qq.com (Y. Pan), 395504090@qq.com (X. Deng), 379925000@qq.com (Y. Qin), zhaoditieren@163.com (D. Zhao), liuzhir8019@126.com (Z. Liu).

<https://doi.org/10.1016/j.heliyon.2024.e35065>

Received 24 November 2023; Received in revised form 20 July 2024; Accepted 22 July 2024

Available online 23 July 2024

2405-8440/© 2024 The Authors. Published by Elsevier Ltd. This is an open access article under the CC BY-NC-ND license (<http://creativecommons.org/licenses/by-nc-nd/4.0/>).

dementia cases [4]. In China, CSVD accounts for 46 % of all ischemic stroke etiologies, with lacunar infarction representing 25%–50 % of these cases [5].

The clinical characteristics of CSVD primarily encompass stroke, cognitive dysfunction, recurrent lacunar infarction, and white matter lesions [1]. Among these, lacunar infarction and parenchymal hemorrhage are more likely to occur during the acute stage, while chronic hypoperfusion leads to continuous and progressive damage to the corresponding brain tissue, resulting in cognitive impairment, dementia, gait abnormalities, movement disorders, urinary retention, mood disturbances, and personality disorders. Due to the insufficiency of clinical signs and symptoms for a definitive diagnosis, neuroimaging plays a crucial role in the diagnosis and management of CSVD patients. Over the past two decades, with the widespread adoption of magnetic resonance technology, neuroimaging characteristics of CSVD have provided a vital foundation for standardized diagnosis and treatment in this field [6]. According to the Standards for Reporting Vascular Changes on Neuroimaging (STRIVE v1) proposed in 2013, neuroimaging features of CSVD include recent small subcortical infarcts, presumed vascular origin lacunes, white matter hyperintensities (WMH), perivascular spaces (PVS), cerebral microbleeds (CMBs), and brain atrophy [7]. However, a single imaging marker cannot fully represent the overall extent of CSVD lesions, and the diagnostic specificity is limited. In 2013, Klarenbeek et al. developed a scale based on four MRI features (asymptomatic lacunar infarcts, WMH, CMBs, and enlarged PVS) to generate a “total CSVD score” ranging from 0 to 4 [8]. This total CSVD burden score can comprehensively reflect the characteristic features of CSVD in the brain, surpassing the consideration of individual characteristics alone [9]. High CSVD burden has been established as a significant risk factor for stroke recurrence, cognitive dysfunction, and emotional disorders [10–12]. However, assessing the total CSVD burden in clinical practice is exceedingly complex. It entails substantial costs to conduct multiple nuclear magnetic resonance (NMR) sequence examinations and necessitates close collaboration between clinicians and imaging specialists, resulting in a considerable time investment for analysis. Consequently, implementing this approach in clinical settings poses challenges. Currently, there is a lack of a straightforward and reliable machine learning (ML) models for swiftly diagnosing the total CSVD burden.

Metabolic syndrome (MetS) is a clinical syndrome characterized by the presence of three or more metabolic risk factors, which include obesity, diabetes or impaired glucose regulation, dyslipidemia, and hypertension [13,14]. In China, due to economic development and lifestyle changes, it is estimated that approximately 454 million people are affected by MetS [15]. However, the existing evidence regarding the association between MetS and CSVD is limited and controversial, particularly concerning the impact of MetS on neuroimaging markers of CSVD. Furthermore, recent studies have indicated that systemic inflammation plays a role in the functioning of the central nervous system (CNS), including the regulation of cerebral blood flow, endothelial function, and blood-brain barrier (BBB) permeability [16]. Previous research has demonstrated a strong link between peripheral inflammation markers and CSVD [17, 18]. Notably, substantial evidence has shown the infiltration of peripheral immune cells in the arteriolar wall and perivascular tissue of CSVD patients [18]. Recently, the complete blood count-derived inflammatory markers, which are composite inflammatory biomarkers calculated using neutrophil, lymphocyte, and platelet counts, have been widely utilized to investigate the associations between systemic inflammation and neurological disorders [19]. However, the correlation between systemic inflammation indicators, such as the neutrophil-to-lymphocyte ratio (NLR), platelet-to-lymphocyte ratio (PLR), systemic immune-inflammation index (SII), and lymphocyte-to-monocyte ratio (LMR), and neuroimaging features of CSVD remains limited.

Our objective is to integrate metabolic and inflammatory indicators to develop a simple ML model that can accurately predict the total CSVD burden. This study collected demographic information, metabolic data, and inflammation-related data to establish a diagnostic model. The predictive performance of six ML models was compared to further analyze the correlation between metabolism, inflammation, and the total burden of CSVD and to select an appropriate model to guide clinical decision-making.

2. Materials and methods

2.1. Study design and participants

Patients with CSVD were recruited from the Neurological Inpatient Department of Xijing Hospital, affiliated with the Fourth Military Medical University, between December 2012 and December 2022. The inclusion criteria for this study were as follows: (1) For patients admitted with first-ever stroke, meeting the diagnostic criteria for CSVD [7]: Upon medical imaging examination, patients exhibit at least one of the following four imaging markers: presumed vascular origin lacunes, WMH, PVS, and CMBs; (2) Age between 18 and 85 years. The exclusion criteria were: (1) Absence of clinical images and laboratory data; (2) Presence of non-CSVD-related white matter lesions (such as multiple sclerosis, encephalitis, poisoning, hydrocephalus, trauma, etc.). Two neurologists with 10 years of clinical experience were involved in collecting patients' demographic characteristics, clinical data, and neuroimaging data and assessing each patient's total CSVD burden score. This study was approved by the Ethics Committee of Xijing Hospital, affiliated with the Fourth Military Medical University (approval number: KY20232227–F-1). We adhered to rigorous ethical standards throughout the research, ensuring that all participating patients and their guardians provided written informed consent. Since no minors were involved in the study, the issue of consent or assent from minors was not applicable.

2.2. Metabolic index evaluation

Comprehensive demographic information, including age and sex, as well as previous medical history, such as diabetes, hypertension, and dyslipidemia, were collected for each patient. Personal lifestyle preferences, including smoking and alcohol consumption, were also recorded. We collected comprehensive examination information of patients with CSVD upon admission, including blood routine parameters, fasting blood glucose (GLU), total cholesterol (TC), low-density lipoprotein (LDL), triglyceride (TG), high-density

lipoprotein (HDL), apolipoprotein A1 (APOA), apolipoprotein B (APOB), uric acid (UA), cystatin C (CysC), albumin, and homocysteine (Hcy) levels.

Age groups were categorized as ≥ 65 years (higher age group) and < 65 years (lower age group). Additionally, APOA, APOB, CysC, and Hcy levels were divided into high and low groups based on the normal range (APOA > 1.2 g/L, APOB < 1.14 g/L, CysC < 1.09 mg/L, Hcy < 15.0 $\mu\text{mol/L}$). All data were collected by trained neurologists at Xijing Hospital, ensuring strict privacy protection of the subjects' information during and after data collection.

Chinese guideline for MetS from the Chinese Diabetes Society was used to define the MetS [20,21]. The specific contents shall comply with 3 or more of the following criteria: (1) Overweight and/or obesity [Body Mass Index (BMI) ≥ 25 kg/m²], (2) hyperglycemia [FPG ≥ 6.1 mmol/L (110 mg/dL) and/or 2h PG ≥ 7.8 mmol/L (140 mg/dl)]; (3) high blood pressure (HBP) (systolic blood pressure ≥ 140 mmHg or diastolic blood pressure ≥ 90 mmHg), (4) dyslipidemia: [fasting plasma TG ≥ 1.7 mmol/L (150 mg/dL), and/or fasting HDL-C < 0.9 mmol/L (35 mg/dl) (male) or < 1.0 mmol/L (39 mg/dl) (female)].

2.3. Complete blood count-derived inflammatory markers evaluation

Fasting blood samples were collected and sent to the laboratory. The absolute counts of white blood cells, neutrophils, monocytes, lymphocytes, and platelets were detected through flow cytometry (XE-2100, SYSMES, Kobe, Japan). Several markers of systemic inflammation were calculated, including NLR (neutrophil count/lymphocyte count), dNLR (neutrophil count/(white blood cell count - neutrophil count)), LMR (lymphocyte count/monocyte count), PLR (platelet count/lymphocyte count), PNI (albumin +5) * lymphocyte count), SII (neutrophil count * platelet count/lymphocyte count), LWR (lymphocyte count/white blood cell count), NWR (neutrophil count/white blood cell count), PNR (platelet count/neutrophil count), SIRI (neutrophil count * monocyte count)/lymphocyte count), and ELR (eosinophil count/lymphocyte count).

2.4. MRI acquisition and assessment

Each CSVD patient underwent a brain MRI scan using a 3.0T MRI scanner (Philips Ingenia 3.0T, Best, Netherlands) with a standardized protocol. The MRI sequences included 3D T1-weighted magnetization-prepared rapid gradient-echo (3D T1w MPRAGE), axial T2-weighted, fluid-attenuated inversion recovery (FLAIR), and axial susceptibility-weighted imaging. CSVD neuroimaging biomarkers were assessed by two neuroradiologists who were well-trained and blinded to the patient's clinical data, following the Standards for Reporting Vascular Changes on Neuroimaging (STRIVE) criteria [7]. WMH was defined as increased brightness in the brain white matter on T2 images. Periventricular and deep WMH were evaluated using the Fazekas scoring system. Lacune was defined as a rounded or ovoid lesion of CSF signal measuring 3–20 mm in diameter. CMBs were defined as circular hypointense lesions measuring 2–10 mm on gradient echo or susceptibility-weighted images. Enlarged perivascular spaces (EPVS) were defined as punctate or linear hyperintensities smaller than 3 mm on T2 images. A total CSVD burden score, ranging from 1 to 4 on an ordinal scale, was calculated based on the previously described and validated criteria by the Wardlaw team. CSVD patients were classified into

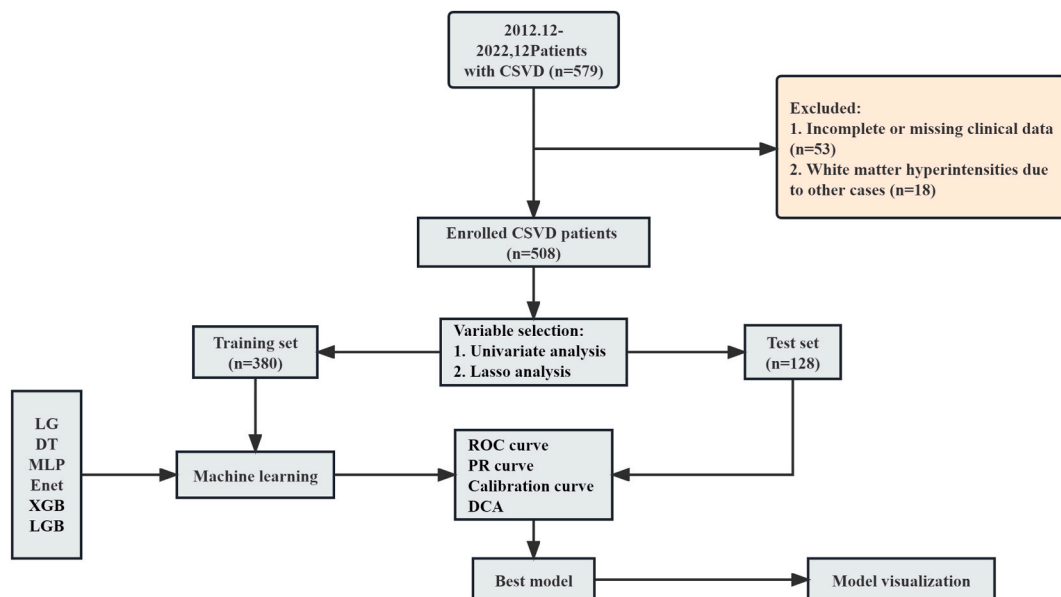


Fig. 1. The flow chart of this study. CSVD: cerebral small vessel disease, LASSO: least absolute shrinkage and selection operator, DT: decision tree; XGB: Extreme Gradient Boosting; Enet: Elastic Net, MLP: Multilayer Perceptron; LGB: Light Gradient Boosting Machine; ROC: receiver operator characteristic, PR: Precision-Recall Curve, DCA: decision curve analysis.

mild and severe groups based on a total CSVD score of ≤ 2 or > 2 .

2.5. Model building

We employed single-factor analysis and lasso regression to select clinical variables and mitigate the issue of multicollinearity. The study population was randomly divided into a training set and a test set, with 75 % of the data allocated to the training set for cross-validation and model tuning and the remaining 25 % used for model validation. Six ML models, including decision tree (DT), Extreme Gradient Boosting (XGBoost), Elastic Net (Enet), Multilayer Perceptron (MLP), Light Gradient Boosting Machine (LightGBM), and logistic regression, were utilized to construct prediction models for comparative analysis. Various metrics such as the area under the receiver operating characteristic curve (ROCauc), the area under the Precision-Recall curve (PRAuc), accuracy, sensitivity, specificity,

Table 1
Baseline characteristic of the study subject.

Variables	Total (n = 508)	Mild (n = 314)	Severe (n = 194)	P
Demographic features				
Male, n (%)	309 (60.8)	187 (59.6)	122 (62.9)	0.513
Age, years	64.00 [55.00, 72.00]	63.00 [53.25, 71.00]	66.50 [58.00, 74.00]	0.004
≥ 65 , n (%)	236 (46.5)	128 (40.8)	108 (55.7)	0.001
< 65 , n (%)	272 (53.5)	186 (59.2)	86 (44.3)	
Smoking, n (%)	171 (33.7)	86 (27.4)	85 (43.8)	< 0.001
Alcohol history, n (%)	116 (22.8)	61 (19.4)	55 (28.4)	0.026
Metabolic related indicators				
Metabolic syndrome, n (%)	194 (38.2)	66 (21.0)	128 (66.0)	< 0.001
Hypertension, n (%)	402 (79.1)	227 (72.3)	175 (90.2)	< 0.001
BMI	24.68 \pm 2.49	24.15 \pm 2.42	25.55 \pm 2.36	< 0.001
Diabetes, n (%)	131 (25.8)	57 (18.2)	74 (38.1)	< 0.001
LDL, mmol/L	2.10 [1.70, 2.74]	2.10 [1.65, 2.63]	2.16 [1.78, 2.85]	0.028
TG, mmol/L	1.23 [0.92, 1.77]	1.17 [0.92, 1.62]	1.29 [0.95, 1.80]	0.044
TC, mmol/L	3.71 [3.14, 4.38]	3.68 [3.13, 4.32]	3.74 [3.21, 4.49]	0.194
HDL, mmol/L	1.05 [0.90, 1.25]	1.10 [0.94, 1.27]	0.96 [0.86, 1.18]	< 0.001
APOA, g/L	1.12 [0.97, 1.28]	1.15 [0.98, 1.31]	1.07 [0.92, 1.22]	0.001
< 1.20 g/L, n (%)	242 (47.6)	128 (40.8)	114 (58.8)	< 0.001
APOB, g/L	0.69 [0.53, 0.86]	0.69 [0.54, 0.87]	0.69 [0.51, 0.86]	0.895
> 1.14 g/L, n (%)	40 (7.9)	20 (6.4)	20 (10.3)	0.152
B.A	0.61 [0.47, 0.78]	0.59 [0.45, 0.76]	0.63 [0.49, 0.83]	0.006
B.L	0.32 [0.28, 0.37]	0.31 [0.27, 0.37]	0.32 [0.28, 0.37]	0.594
A.H	1.04 [0.93, 1.16]	1.03 [0.94, 1.15]	1.06 [0.92, 1.18]	0.359
UA, μ mol/L	292.00 [238.00, 354.00]	282.00 [232.00, 334.00]	312.00 [258.25, 371.00]	< 0.001
CysC, μ mol/L	1.06 [0.93, 1.20]	1.02 [0.89, 1.16]	1.13 [0.96, 1.25]	< 0.001
> 1.09 mg/L, n (%)	221 (43.5)	108 (34.4)	113 (58.2)	< 0.001
Hcy, μ mol/L	13.88 [9.80, 19.38]	12.31 [9.03, 16.98]	16.91 [12.52, 21.20]	< 0.001
> 15.0 μ mol/L, n (%)	222 (43.7)	100 (31.8)	122 (62.9)	< 0.001
Systemic Inflammatory markers				
Neutrophils, $\times 10^9/L$	3.67 [2.74, 4.60]	3.46 [2.59, 4.32]	3.99 [3.20, 5.24]	< 0.001
Lymphocytes, $\times 10^9/L$	1.69 [1.31, 2.04]	1.75 [1.42, 2.09]	1.60 [1.21, 1.96]	< 0.001
Platelets, $\times 10^9/L$	193.50 [159.00, 236.00]	197.50 [161.00, 238.75]	189.00 [157.50, 231.75]	0.335
WBC, $\times 10^9/L$	6.06 [4.87, 7.31]	5.91 [4.64, 7.12]	6.43 [5.25, 7.56]	0.002
Monocyte, $\times 10^9/L$	0.41 [0.32, 0.51]	0.40 [0.32, 0.51]	0.42 [0.33, 0.54]	0.102
Eosinophils, $\times 10^9/L$	0.10 [0.07, 0.18]	0.11 [0.07, 0.18]	0.10 [0.06, 0.18]	0.556
Basophils, $\times 10^9/L$	0.02 [0.01, 0.04]	0.02 [0.01, 0.03]	0.02 [0.01, 0.04]	0.737
LMR	4.12 [2.95, 5.24]	4.38 [3.35, 5.58]	3.64 [2.68, 4.77]	< 0.001
PNI	48.05 [44.64, 51.15]	48.38 [45.42, 51.81]	47.25 [43.20, 49.95]	< 0.001
SIRI	0.87 [0.59, 1.37]	0.78 [0.53, 1.19]	1.06 [0.70, 1.68]	< 0.001
dNLR	1.54 [1.15, 2.07]	1.41 [1.10, 1.96]	1.81 [1.31, 2.36]	< 0.001
NLR	2.08 [1.52, 2.92]	1.86 [1.43, 2.60]	2.57 [1.87, 3.78]	< 0.001
PLR	116.17 [91.56, 148.43]	114.01 [90.09, 143.87]	119.90 [96.75, 161.90]	0.014
SII	407.93 [276.58, 612.22]	375.89 [259.02, 539.26]	479.91 [323.76, 755.90]	< 0.001
ELR	0.06 [0.04, 0.11]	0.06 [0.04, 0.11]	0.07 [0.04, 0.12]	0.526
LWR	0.29 [0.22, 0.35]	0.31 [0.24, 0.36]	0.25 [0.20, 0.31]	< 0.001
NWR	0.61 [0.54, 0.68]	0.59 [0.53, 0.66]	0.64 [0.57, 0.71]	< 0.001
PNR	52.97 [40.11, 70.61]	56.10 [42.40, 73.46]	48.33 [35.61, 63.50]	< 0.001

Abbreviations: Values for continuous variables are expressed as mean \pm standard deviation or interquartile range; values for categorical data are given as numbers (percent). Mild: CSVD (Cerebral Small Vessel Disease) total burden score ≤ 2 points. Severe: CSVD total burden score > 2 points. B.A: APOB/APOA. B.L: APOB/LDL. A.H: APOA/HDL, NLR: Neutrophil Count/Lymphocyte Count, dNLR: Neutrophil Count/(White Blood Cell Count - Neutrophil Count), LMR: Lymphocyte Count/Monocyte Count, PLR: Platelet Count/Lymphocyte Count, PNI: Albumin + 5 * Lymphocyte Count, SII: Neutrophil Count * Platelet Count/Lymphocyte Count, LWR: Lymphocyte Count/White Blood Cell Count, NWR: Neutrophil Count/White Blood Cell Count, PNR: Platelet Count/Neutrophil Count, SIRI: (Neutrophil Count * Monocyte Count)/Lymphocyte Count, ELR: Eosinophil Count/Lymphocyte Count, p values are compared between Mild and Severe groups.

positive predictive value (PPV), negative predictive value (NPV), f-measure, kappa, calibration curve, and decision curve analysis (DCA) curve were employed to evaluate the prediction performance and clinical applicability. The Shapley Additive explanation (SHAP) method was used to assess the importance of features in the model, and the interpretability of the model was demonstrated through shapley feature importance ranking and SHAP summary diagrams [22]. Select the best model and make a web calculator based on the shiny package. The tidymodels package (version 1.1.0) in R (version 4.3.0) was employed for training and comparing different ML models. The entire study design is depicted in Fig. 1.

2.6. Statistics

Continuous variables were expressed as median (P25, P75) and categorical variables were expressed as counts and percentages. Mann-Whitney *U* test and Fisher exact test were used to compare baseline characteristics between the two groups. $P < 0.05$ was considered statistically significant.

3. Result

3.1. Clinical characteristics of CSVD patients

A total of 579 patients diagnosed with CSVD were enrolled in this study, with 508 patients meeting the Inclusion criteria. Among these, 314 cases were classified as mild CSVD, and 194 cases were categorized as severe CSVD. In the mild CSVD group, 128 patients (40.8 %) were aged 65 years or older, and the male-to-female ratio was 59.6 %. In the severe CSVD group, 108 patients (55.7 %) were aged 65 years or older, with males accounting for 62.9 %. Notably, there was a statistically significant difference in age distribution between the two groups [Table 1].

3.2. Feature selection

In the univariate analysis, 38 factors related to demographic information, metabolic and systemic inflammation markers were included for analysis [Table 1]. The results revealed significant differences in various factors between the mild and severe CSVD groups. These factors included age, MetS, hypertension, smoking, diabetes, alcohol consumption, BMI, LDL, TG, HDL, APOA, B.A, UA, CysC, Hcy, Neutrophil count (N), Lymphocyte count (L), White Blood Cell count (WBC), LMR, PNI, SIRI, dNLR, NLR, PLR, SII, ELR, NWR, and PNR.

The meaningful variables identified in the single-factor analysis were further subjected to lasso regression for variable screening to address multicollinearity. Based on the sparse matrix obtained, the lasso regression selected the following characteristics: age, smoking, MetS, UA, CysC, Hcy, NLR, and PNI. These eight variables were then retained as inputs for the model design [Fig. 2A and B].

3.3. Multiple ML models comparison

For the prediction of total CSVD burden, among the six ML models, logistic regression demonstrated the highest value (ROCauc = 0.8494), while DT exhibited the lowest area under the receiver operating characteristic curve value (ROCauc = 0.7771) (Fig. 3A). In terms of the area under the PRAuc, logistic regression achieved the highest PRAuc (PRAuc = 0.8071), while DT had the lowest value among the six ML models (PRAuc = 0.7248) (Fig. 3B). Furthermore, logistic regression outperformed other ML models in terms of calibration, as indicated by the Brier score (BS = 0.146), and showed a better fit to the ideal calibration curve (gray dashed line)

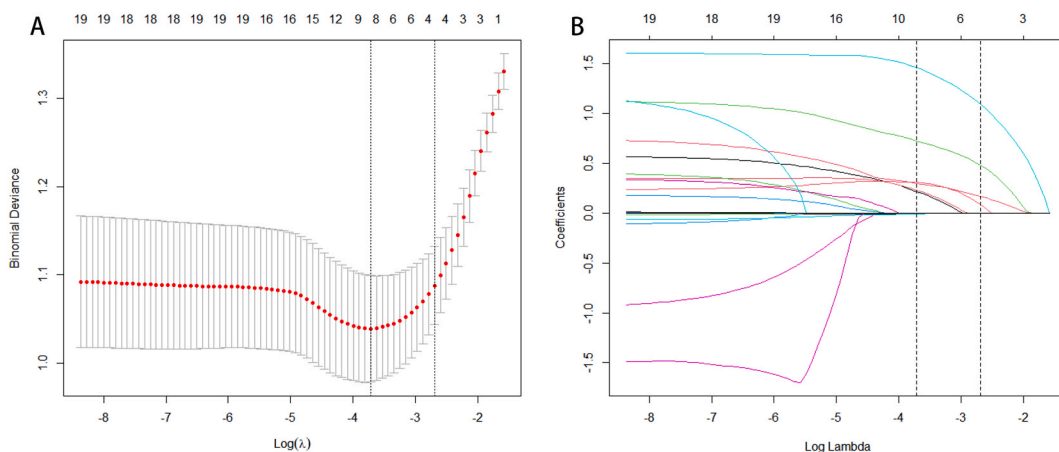


Fig. 2. LASSO regression analysis screened the feature variables. (A) The misclassification error in the jackknife rate analysis. (B) LASSO coefficient profiles.

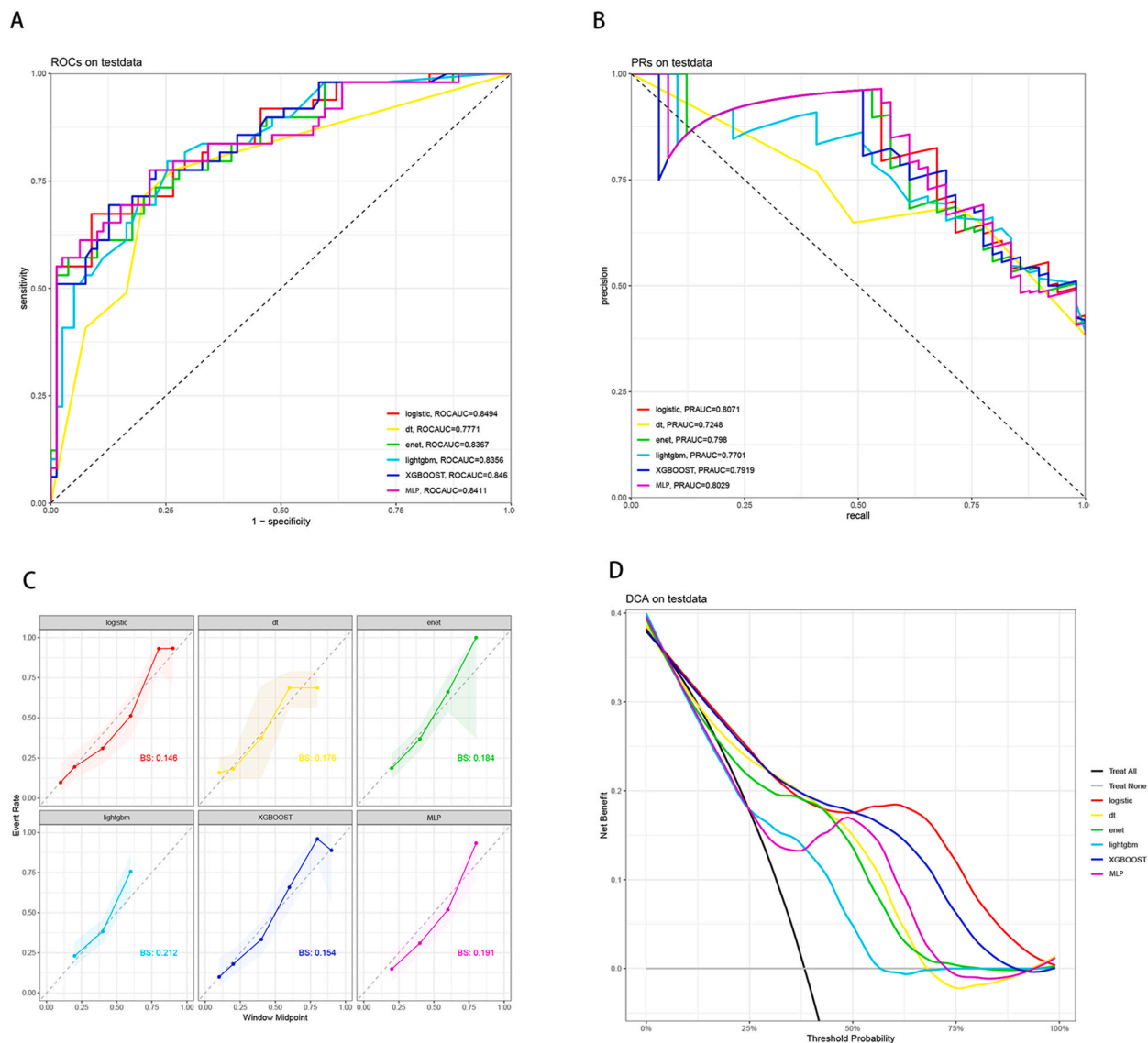


Fig. 3. Predictive performance of six machine learning models for metabolic syndromes and systemic inflammation index with neuroimaging burden of CSVD in test data. (A) The receiver operating characteristic curve (ROCAuc) curve of six machine learning models. (B) The area under the Precision-Recall curve (PRAuc) of six machine learning models. (C) The calibration curve of six machine learning models. (D) The decision curve analysis (DCA) of six machine learning models.

Table 2
Comparison of six machine learning models for CSVD neuroimaging load prediction.

model	accuracy	kap	sens	spec	ppv	npv	mcc	precision	f_meas	roc_auc	pr_auc
logistic	0.773	0.519	0.694	0.823	0.708	0.813	0.519	0.708	0.701	0.849	0.807
dt	0.766	0.508	0.714	0.797	0.686	0.818	0.508	0.686	0.700	0.777	0.725
enet	0.750	0.479	0.714	0.772	0.660	0.813	0.480	0.660	0.686	0.837	0.798
lightgbm	0.750	0.479	0.714	0.772	0.660	0.813	0.480	0.660	0.686	0.836	0.770
XGBOOST	0.758	0.493	0.714	0.785	0.673	0.816	0.494	0.673	0.693	0.846	0.792
SLP	0.742	0.481	0.796	0.709	0.629	0.848	0.491	0.629	0.703	0.841	0.803

DT: decision tree; XGBoost: Extreme Gradient Boosting; Enet: Elastic Net, SLP: Single-Layer Perceptron; LightGBM: Light Gradient Boosting Machine; kap: Kappa coefficient, sens: Sensitivity, spec: Specificity, ppv: Positive predictive value, npv: Negative, predictive value, mcc: Matthews correlation coefficient, precision: Precision, f_meas: F1 score, roc_auc: Area under the ROC curve, pr_auc: Area under the precision-recall curve.

(Fig. 3C). The DCA curve indicated no significant difference in net benefit between the six ML models within the range of 0%–25 % threshold probability. However, from 25 % to 50 %, logistic regression demonstrated the greatest net benefit when combined with XGboost. Additionally, from 50 % to 100 %, logistic regression exhibited the greatest net benefit (Fig. 3D). In conclusion, based on our findings, we considered logistic regression to be the optimal model among the six ML models. The performance of six ML models is shown in Table 2.

3.4. Model interpretability

The importance ranking diagram generated by logistic regression for SHAP features reveals that MetS, NLR, and Hcy were the top three significant features (Fig. 4A). SHAP summary plots illustrated that each feature positively or negatively predicted a high total negative CSVD. Each dot on the plot represented an individual's eigenvalue (SHAP value), with the color indicating the magnitude of the eigenvalue (red dots indicate lower values, while blue dots indicate higher values). SHAP calculated the total SHAP value for each individual, and a higher total SHAP value indicated an increased likelihood of a high CSVD burden. Specifically, concerning MetS, the blue dots were prominently clustered on the right side of the graph, suggesting that the total SHAP value for CSVD high burden was elevated in the presence of MetS (Fig. 4B).

3.5. Model visualization

This study utilized a logistic regression model and Rshiny to develop interactive web calculators. These calculators can be accessed directly through the website <https://neurology.shinyapps.io/Shiny4Burden/>. By inputting the clinical features of CSVD patients, the calculators can compute the probability of a high CSVD imaging burden. For instance, consider a CSVD patient with metabolic syndrome, a smoking history, Hcy level greater than 15.0 $\mu\text{mol/L}$, CysC level greater than 1.09 mg/L, age greater than or equal to 65 years, UA level of 300, PNI of 40.15, NLR of 2.25, and so on. Upon clicking “predict,” the calculator will compute the probability of a high CSVD imaging burden, which in this case is 0.8141 (Fig. 5).

4. Discussion

In the study of CSVD total burden scores, various methodologies have been proposed to enhance the accuracy and practicality of these assessments. This study utilizes the classic score by Staals et al. [9], based on lacunes, WMH, CMBs, and EPVS with a maximum of 4 points, significantly predicting cardiovascular events, stroke, and cognitive decline. Lau et al. [23] modified the system, raising the PVS threshold to >20 for 1 point and adding CMBs and Fazekas sub-scores, yielding a 6-point score. This new system matches the classic for stroke recurrence prediction but better identifies high-risk intracerebral hemorrhage (ICH) patients. Pasi et al. [24] found the 6-point score excels in predicting post-ICH cognitive impairment. Moreover, research has shown that even after excluding WMH from the scoring system, it remains associated with overall cognitive dysfunction, though not with processing or memory functions [25]. Kim et al. [26] further revised the CSVD total burden score by removing the PVS component, resulting in a simplified 0–3 scale, which demonstrated that in patients with subcortical vascular cognitive impairment (SVCI), increased $A\beta$ and CSVD burden were independently correlated with tau protein accumulation, suggesting that CSVD burden can independently drive tau deposition, irrespective of $A\beta$ status. Although this study did not directly compare with the classic scoring system, it provides significant pathophysiological insights into the mechanisms of SVCI and tau deposition patterns. Summarizing different systems, Lau et al.'s modified system proves more valuable in identifying high-risk ICH patients, while Staals' classic score remains more user-friendly for clinical practice. Additionally, STRIVE-2 has incorporated newly identified imaging markers such as cortical superficial siderosis (cSS) and

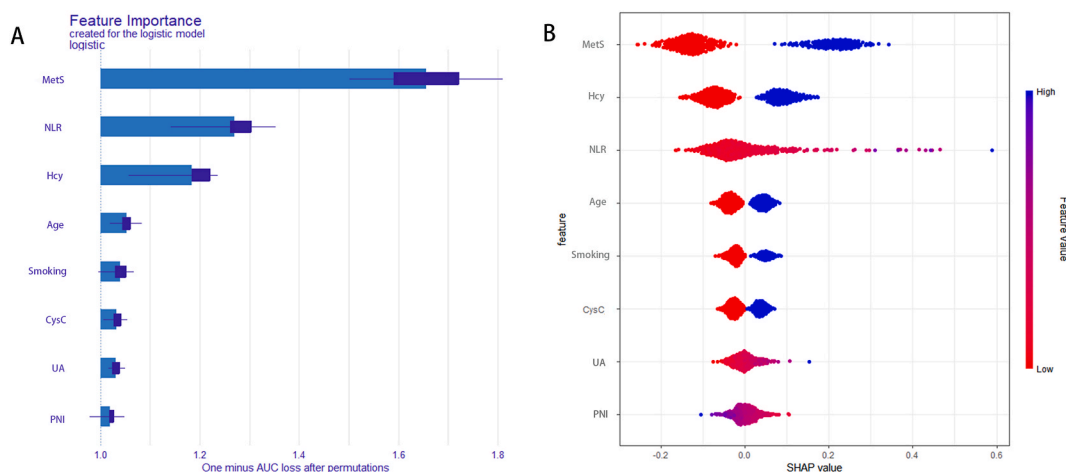


Fig. 4. Feature importance of logistic regression. (A) Feature importance of logistic regression. (B) SHAP value of 8 variables.

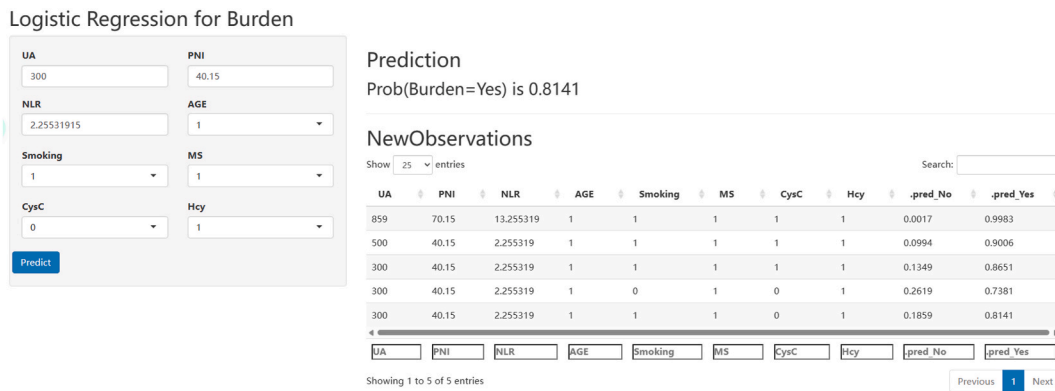


Fig. 5. The interactive web calculators based on logistic regression model.

cortical cerebral microinfarcts (CMI), enhancing the comprehensive assessment of CSVD total burden [27].

Based on the classical CSVD scoring system, this study utilized various machine learning methods to explore the relationship between MetS, complete blood count-derived inflammatory markers, and the neuroimaging burden of CSVD. Through univariate and LASSO analyses, eight variables, including age, smoking, MetS, UA, CysC, Hcy, NLR and PNI, were identified as critical factors influencing the imaging burden of CSVD. Subsequently, six ML methods, including Enet, logistic regression, MLP, DT, XGBoost and LightGBM, were employed to construct a prediction model for the neuroimaging burden of CSVD. Following training data model construction and test data validation, the logistic regression model demonstrated the best performance in predicting the neuroimaging burden of CSVD. In the logistic regression feature significance analysis, MetS and NLR were identified as the most essential factors in the neuroimaging burden of CSVD. These web-based calculators based on the developed models can be applied in clinical practice to assist clinicians in efficiently diagnosing the total burden of cerebrovascular diseases, thereby reducing examination costs and consultation time for patients.

MetS and complete blood count-derived inflammatory markers have been found to be closely associated with CSVD [15,16]. While previous studies have focused on the relationship between CSVD and MetS or complete blood count-derived inflammatory markers, There has been limited research exploring the association between MetS, complete blood count-derived inflammatory markers, and the total imaging burden of CSVD.

In previous studies, MetS has been shown to be independently associated with the prevalence of periventricular white matter lesions and deep white matter lesions in middle-aged and elderly patients [28]. In 2021, Shu et al. conducted a community-based study to investigate the relationship between MetS and CSVD [15]. They found that the severity of MetS was significantly associated with higher risks of WMH volume and lacunes, but not with the presence of cerebral CMBs and PVS severity [15]. In CSVD patients, MetS was found to be related to worse pre-existing cognitive impairment and depression [29]. Therefore, MetS is considered as one of the critical factors influencing the pathological characteristics and clinical manifestations of CSVD. However, the underlying mechanism by which MetS contributes to the development of CSVD still needs to be fully understood. For example, hyperlipoproteinemia and hypertension may impair neuronal nutrition and oxygenation through increased vascular permeability [29]. Additionally, insulin resistance can disrupt cerebrovascular reactivity [29]. Further studies are needed to elucidate the mechanisms underlying the influence of MetS on CSVD.

Recently, there have been several studies exploring the relationship between inflammation and CSVD [30,31]. The systemic immune-inflammation index (SII), a novel biomarker of systemic inflammation, comprehensively reflects the systemic inflammatory status and immune response [32,33]. In 2022, Jiang et al. investigated the association between neutrophil count (NC), NLR, SII, and CSVD. They found that NC was associated with moderate-to-severe basal ganglia EPVS and lacunes in a community-based population [16]. Furthermore, a recent observational study demonstrated that elevated NLR was correlated with more severe WMH, microbleeds, and lacunes in CSVD [30]. Similarly, an increased SII index, calculated as platelet count multiplied by neutrophil count divided by lymphocyte count, was found to be associated with a higher burden of severe CSVD [34]. These findings are consistent with the results of our study. In this study, Hcy has also been identified as an essential contributor to CSVD neuroimaging burden. Previous studies have indicated the potential role of homocysteine on the risk of lacunes, WMH, CBMS and EPVS [35–38]. A recent mendelian randomization study showed that total Hcy level was related with CSVD imaging burden, including brain volume loss and lacunes [39]. Therefore, the results of a series of studies, including this one, support an important association of Hcy with CSVD neuroimaging burden risk. In molecular mechanisms, preclinical and clinical research demonstrated that Hcy took part in the pathological process of CSVD through damaging endothelial cell function, promoting oxidative stress and neuroinflammation [17,40–42].

This study also has several limitations. Firstly, it is based on cross-sectional data, and the analysis of prospective data is lacking. Secondly, the data were obtained from a single research center, and the sample size was relatively small. External validation of the model using data from different regions would enhance its stability and applicability.

5. Conclusion

In summary, this study constructed a prediction system based on metabolic and complete blood count-derived inflammatory markers to predict the neuroimaging burden of CSVD patients through 6 ML methods. Among them, logistic regression had the best comprehensive performance and can accurately predict the imaging burden level of CSVD patients. Future studies can focus on the effects of metabolic and inflammatory factors on the disease progression in patients with CSVD.

Data availability statement

Due to the sensitive nature of the data used in this study, they are not publicly available. Data are however available from the corresponding author upon reasonable request and with permission of the Ethics Committee of Affiliated Xijing Hospital of Fourth Military Medical University.

Ethics approval

The experimental protocol was approved by the Ethics Committee of Affiliated Xijing Hospital of Fourth Military Medical University (approval number: KY20232227–F-1). We adhered to rigorous ethical standards throughout the research, ensuring that all participating patients and their guardians provided written informed consent. Since no minors were involved in the study, the issue of consent or assent from minors was not applicable.

Consent for publication

Not applicable.

Funding

This work was supported by the National Key Research and Development Program of China (No. 2017YFC0907703).

CRediT authorship contribution statement

Yang Wang: Writing – original draft, Software, Formal analysis, Data curation. **Yang Li:** Supervision, Investigation, Data curation. **Shusheng Jiao:** Software, Methodology, Data curation. **Yuanhang Pan:** Visualization, Software, Formal analysis. **Xiwei Deng:** Formal analysis, Data curation. **Yunlong Qin:** Formal analysis, Data curation. **Di Zhao:** Software, Investigation. **Zhirong Liu:** Writing – review & editing, Supervision, Funding acquisition, Conceptualization.

Declaration of competing interest

The authors declare that they have no known competing financial interests or personal relationships that could have appeared to influence the work reported in this paper.

Acknowledgments

Not applicable.

References

- [1] B. Ren, L. Tan, Y. Song, D. Li, B. Xue, X. Lai, Y. Gao, Cerebral small vessel disease: neuroimaging features, biochemical markers, influencing factors, pathological mechanism and treatment, *Eng. Epub* 2022/07/02, *Front. Neurol.* 13 (2022) 843953, <https://doi.org/10.3389/fneur.2022.843953>. Cited in: Pubmed; PMID 35775047.
- [2] R.J. Cannistraro, M. Badi, B.H. Eidelman, D.W. Dickson, E.H. Middlebrooks, J.F. Meschia, CNS small vessel disease: a clinical review, *Eng. Epub* 2019/05/31, *Neurology* 92 (24) (2019 Jun 11) 1146–1156, <https://doi.org/10.1212/wnl.0000000000007654>. Cited in: Pubmed; PMID 31142635.
- [3] G.W. Petty, R.D. Brown Jr., J.P. Whisnant, J.D. Sicks, W.M. O'Fallon, D.O. Wiebers, Ischemic stroke subtypes: a population-based study of functional outcome, survival, and recurrence, *Eng. Epub* 2000/05/08, *Stroke* 31 (5) (2000 May) 1062–1068, <https://doi.org/10.1161/01.str.31.5.1062>. Cited in: Pubmed; PMID 10797166.
- [4] J.M. Wardlaw, C. Smith, M. Dichgans, Small vessel disease: mechanisms and clinical implications, *Eng. Epub* 2019/05/18, *Lancet Neurol.* 18 (7) (2019 Jul) 684–696, [https://doi.org/10.1016/s1474-4422\(19\)30079-1](https://doi.org/10.1016/s1474-4422(19)30079-1). Cited in: Pubmed; PMID 31097385.
- [5] J.M. Wardlaw, C. Smith, M. Dichgans, Mechanisms of sporadic cerebral small vessel disease: insights from neuroimaging, *Eng. Epub* 2013/04/23, *Lancet Neurol.* 12 (5) (2013 May) 483–497, [https://doi.org/10.1016/s1474-4422\(13\)70060-7](https://doi.org/10.1016/s1474-4422(13)70060-7). Cited in: Pubmed; PMID 23602162.
- [6] L. Pantoni, Cerebral small vessel disease: from pathogenesis and clinical characteristics to therapeutic challenges, *Eng. Epub* 2010/07/09, *Lancet Neurol.* 9 (7) (2010 Jul) 689–701, [https://doi.org/10.1016/s1474-4422\(10\)70104-6](https://doi.org/10.1016/s1474-4422(10)70104-6). Cited in: Pubmed; PMID 20610345.
- [7] J.M. Wardlaw, E.E. Smith, G.J. Biessels, C. Cordonnier, F. Fazekas, R. Frayne, R.I. Lindley, J.T. O'Brien, F. Barkhof, O.R. Benavente, S.E. Black, C. Brayne, M. Breteler, H. Chabriat, C. Decarli, F.E. de Leeuw, F. Doubal, M. Duering, N.C. Fox, S. Greenberg, V. Hachinski, I. Kilimann, V. Mok, R. Oostenbrugge, L. Pantoni, O. Speck, B.C. Stephan, S. Teipel, A. Viswanathan, D. Werring, C. Chen, C. Smith, M. van Buchem, B. Norrving, P.B. Gorelick, M. Dichgans, Neuroimaging standards for research into small vessel disease and its contribution to ageing and neurodegeneration, 38. *Eng. Epub* 2013/07/23, *Lancet Neurol.* 12 (8) (2013 Aug) 822, [https://doi.org/10.1016/s1474-4422\(13\)70124-8](https://doi.org/10.1016/s1474-4422(13)70124-8). Cited in: Pubmed; PMID 23867200.

- [8] P. Klarenbeek, R.J. van Oostenbrugge, R.P. Rouhl, I.L. Knottnerus, J. Staals, Ambulatory blood pressure in patients with lacunar stroke: association with total MRI burden of cerebral small vessel disease, *eng. Epub* 2013/08/29, *Stroke* 44 (11) (2013 Nov) 2995–2999, <https://doi.org/10.1161/strokeaha.113.002545>. Cited in: Pubmed; PMID 23982717.
- [9] J. Staals, S.D. Makin, F.N. Doubal, M.S. Dennis, J.M. Wardlaw, Stroke subtype, vascular risk factors, and total MRI brain small-vessel disease burden, *eng. Epub* 2014/08/29, *Neurology* 83 (14) (2014 Sep 30) 1228–1234, <https://doi.org/10.1212/wnl.0000000000000837>. Cited in: Pubmed; PMID 25165388.
- [10] M. Hosoya, S. Toi, M. Seki, M. Saito, T. Hoshino, H. Yoshizawa, K. Kitagawa, Association between total cerebral small vessel disease score and cognitive function in patients with vascular risk factors, *eng. Epub* 2023/03/10, *Hypertens. Res.* : official journal of the Japanese Society of Hypertension 46 (5) (2023 May) 1326–1334, <https://doi.org/10.1038/s41440-023-01244-8>. Cited in: Pubmed; PMID 36894746.
- [11] X. Wang, J. Lyu, Z. Meng, X. Wu, W. Chen, G. Wang, Q. Niu, X. Li, Y. Bian, D. Han, W. Guo, S. Yang, X. Bian, Y. Lan, L. Wang, Q. Duan, T. Zhang, C. Duan, C. Tian, L. Chen, X. Lou, Small vessel disease burden predicts functional outcomes in patients with acute ischemic stroke using machine learning, *eng. Epub* 2023/01/18, *CNS Neurosci. Ther.* 29 (4) (2023 Apr) 1024–1033, <https://doi.org/10.1111/cns.14071>. Cited in: Pubmed; PMID 36650639.
- [12] M.K. Georgakis, R. Fang, M. Düring, F.A. Wollenweber, F.J. Bode, S. Stösser, C. Kindlein, P. Hermann, T.G. Liman, C.H. Nolte, L. Kerti, B. Ikenberg, K. Bernkopf, H. Poppert, W. Glanz, V. Perosa, D. Janowitz, M. Wagner, K. Neumann, O. Speck, L. Dobisch, E. Düzel, B. Gesierich, A. Dewenter, A. Spottke, K. Waegemann, M. Görtler, S. Wunderlich, M. Endres, I. Zerr, G. Petzold, M. Dichgans, Cerebral small vessel disease burden and cognitive and functional outcomes after stroke: a multicenter prospective cohort study, *eng. Epub* 2022/07/26, *Alzheimer's Dementia : the journal of the Alzheimer's Association* 19 (4) (2023 Apr) 1152–1163, <https://doi.org/10.1002/alz.12744>. Cited in: Pubmed; PMID 35876563.
- [13] P.L. Huang, A comprehensive definition for metabolic syndrome, *eng. Epub* 2009/05/02, *Disease models & mechanisms* 2 (5–6) (2009 May-Jun) 231–237, <https://doi.org/10.1242/dmm.001180>. Cited in: Pubmed; PMID 19407331.
- [14] K.G. Alberti, R.H. Eckel, S.M. Grundy, P.Z. Zimmet, J.I. Cleeman, K.A. Donato, J.C. Fruchart, W.P. James, C.M. Loria, S.C. Smith Jr., Harmonizing the metabolic syndrome: a joint interim statement of the international diabetes federation task force on epidemiology and prevention; national heart, lung, and blood institute; American heart association; world heart federation; international atherosclerosis society; and international association for the study of obesity, *eng. Epub* 2009/10/07, *Circulation* 120 (16) (2009 Oct 20) 1640–1645, <https://doi.org/10.1161/circulationaha.109.192644>. Cited in: Pubmed; PMID 19805654.
- [15] M.J. Shu, F.F. Zhai, D.D. Zhang, F. Han, L. Zhou, J. Ni, M. Yao, S.Y. Zhang, L.Y. Cui, Z.Y. Jin, H.J. Zhu, Y.C. Zhu, Metabolic syndrome, intracranial arterial stenosis and cerebral small vessel disease in community-dwelling populations, *Epub* 2021/04/28, *Stroke and vascular neurology* 6 (4) (2021 Dec) 589–594, <https://doi.org/10.1136/svn-2020-000813>. Cited in: Pubmed; PMID 33903177.
- [16] L. Jiang, X. Cai, D. Yao, J. Jing, L. Mei, Y. Yang, S. Li, A. Jin, X. Meng, H. Li, T. Wei, Y. Wang, Y. Pan, Y. Wang, Association of inflammatory markers with cerebral small vessel disease in community-based population, *eng. Epub* 2022/05/06, *J. Neuroinflammation* 19 (1) (2022 May 6) 106, <https://doi.org/10.1186/s12974-022-02468-0>. Cited in: Pubmed; PMID 35513834.
- [17] A. Low, E. Mak, J.B. Rowe, H.S. Markus, J.T. O'Brien, Inflammation and cerebral small vessel disease: a systematic review, *eng. Epub* 2019/06/11, *Ageing Res. Rev.* 53 (2019 Aug) 100916, <https://doi.org/10.1016/j.arr.2019.100916>. Cited in: Pubmed; PMID 31181331.
- [18] Y. Fu, Y. Yan, Emerging role of immunity in cerebral small vessel disease, *eng. Epub* 2018/02/10, *Front. Immunol.* 9 (2018) 67, <https://doi.org/10.3389/fimmu.2018.00067>. Cited in: Pubmed; PMID 29422904.
- [19] O.H. Del Brutto, R.M. Mera, D.A. Rumbaa, V.J. Del Brutto, Systemic immune-inflammation index and progression of white matter hyperintensities of presumed vascular origin. A longitudinal population study in community-dwelling older adults living in rural Ecuador, *eng. Epub* 2023/07/29 21:48, *J. Neurol. Sci.* 452 (2023 Jul 24) 120741, <https://doi.org/10.1016/j.jns.2023.120741>. Cited in: Pubmed; PMID 37515846.
- [20] C. Pang, L. Jia, X. Hou, S. Gao, W. Liu, Y. Bao, W. Jia, The significance of screening for microvascular diseases in Chinese community-based subjects with various metabolic abnormalities, *eng. Epub* 2014/05/20, *PLoS One* 9 (5) (2014) e97928, <https://doi.org/10.1371/journal.pone.0097928>. Cited in: Pubmed; PMID 24835219.
- [21] W. Xu, Z. Zhang, K. Hu, P. Fang, R. Li, D. Kong, M. Xuan, Y. Yue, D. She, Y. Xue, Identifying metabolic syndrome easily and cost effectively using non-invasive methods with machine learning models, *eng. Epub* 2023/07/24, *Diabetes, Metab. Syndrome Obes. Targets Ther.* 16 (2023) 2141–2151, <https://doi.org/10.2147/DMSO.S413829>. Cited in: Pubmed; PMID 37484515.
- [22] S.M. Lundberg, G. Erion, H. Chen, A. DeGrave, J.M. Prutkin, B. Nair, R. Katz, J. Himmelfarb, N. Bansal, S.I. Lee, From local explanations to global understanding with explainable AI for trees, *eng. Epub* 2020/07/02, *Nat. Mach. Intell.* 2 (1) (2020 Jan) 56–67, <https://doi.org/10.1038/s42256-019-0138-9>. Cited in: Pubmed; PMID 32607472.
- [23] K.K. Lau, L. Linxin, U. Schulz, et al., Total small vessel disease score and risk of recurrent stroke: validation in 2 large cohorts, *eng. Epub* 2017/05/12, *Neurology* 88 (24) (2017 Jun 13) 2260–2267, <https://doi.org/10.1212/WNL.0000000000004042>. Cited in: Pubmed; PMID 28515266.
- [24] M. Pasi, L. Sugita, L. Xiong, et al., Association of cerebral small vessel disease and cognitive decline after intracerebral hemorrhage, *eng. Epub* 2020/11/25, *Neurology* 96 (2) (2021 Jan 12) e182–e192, <https://doi.org/10.1212/WNL.0000000000011050>. Cited in: Pubmed; PMID 33067403.
- [25] J. Staals, T. Booth, Z. Morris, et al., Total MRI load of cerebral small vessel disease and cognitive ability in older people, *eng. Epub* 2015/07/04, *Neurobiol. Ageing* 36 (10) (2015 Oct) 2806–2811, <https://doi.org/10.1016/j.neurobiolaging.2015.06.024>. Cited in: Pubmed; PMID 26189091.
- [26] H.J. Kim, S. Park, H. Cho, et al., Assessment of extent and role of tau in subcortical vascular cognitive impairment using 18F-AV1451 positron emission tomography imaging, *eng. Epub* 2018/06/12, *JAMA Neurol.* 75 (8) (2018 Aug 1) 999–1007, <https://doi.org/10.1001/jamaneurol.2018.0975>. Cited in: Pubmed; PMID 29799981.
- [27] M. Düring, G.J. Biesels, A. Brodtmann, et al., Neuroimaging standards for research into small vessel disease—advances since 2013, *eng. Epub* 2023/06/20, *Lancet Neurol.* 22 (7) (2023 Jul) 602–618, [https://doi.org/10.1016/S1474-4422\(23\)00131-X](https://doi.org/10.1016/S1474-4422(23)00131-X). Cited in: Pubmed; PMID 37236211.
- [28] Z.G. Yin, M. Cui, S.M. Zhou, M.M. Yu, R. Li, H.D. Zhou, Association between metabolic syndrome and white matter lesions in middle-aged and elderly patients, *eng. Epub* 2014/04/05, *Eur. J. Neurol.* 21 (7) (2014 Jul) 1032–1039, <https://doi.org/10.1111/ene.12433>. Cited in: Pubmed; PMID 24698428.
- [29] T.B. Matic, G. Toncevic, A. Gavrilović, D. Aleksić, Suffering from cerebral small vessel disease with and without metabolic syndrome, *eng. Epub* 2019/06/25, *Open Med.* 14 (2019) 479–484, <https://doi.org/10.1515/med-2019-0051>. Cited in: Pubmed; PMID 31231684.
- [30] S.Y. Chuang, Y.C. Hsu, K.W. Chou, K.S. Chang, C.H. Wong, Y.H. Hsu, H.M. Cheng, C.W. Chen, P.Y. Chen, Neutrophil-lymphocyte ratio as a predictor of cerebral small vessel disease in a geriatric community: the I-lan longitudinal aging study, *Epub* 2023/07/29, *Brain Sci.* 13 (7) (2023 Jul 18) <https://doi.org/10.3390/brainsci13071087>. Cited in: Pubmed; PMID 37509017.
- [31] L.E. Evans, J.L. Taylor, C.J. Smith, H.A.T. Pritchard, A.S. Greenstein, S.M. Allan, Cardiovascular comorbidities, inflammation, and cerebral small vessel disease, *eng. Epub* 2021/09/10, *Cardiovasc. Res.* 117 (13) (2021 Nov 22) 2575–2588, <https://doi.org/10.1093/cvr/cvab284>. Cited in: Pubmed; PMID 34499123.
- [32] B. Hu, X.R. Yang, Y. Xu, Y.F. Sun, C. Sun, W. Guo, X. Zhang, W.M. Wang, S.J. Qiu, J. Zhou, J. Fan, Systemic immune-inflammation index predicts prognosis of patients after curative resection for hepatocellular carcinoma, *eng. Epub* 2014/10/02, *Clin. Cancer Res.* : an official journal of the American Association for Cancer Research 20 (23) (2014 Dec 1) 6212–6222, <https://doi.org/10.1158/1078-0432.Ccr-14-0442>. Cited in: Pubmed; PMID 25271081.
- [33] Z. Ye, T. Hu, J. Wang, R. Xiao, X. Liao, M. Liu, Z. Sun, Systemic immune-inflammation index as a potential biomarker of cardiovascular diseases: a systematic review and meta-analysis, *eng. Epub* 2022/08/26, *Frontiers in cardiovascular medicine* 9 (2022) 933913, <https://doi.org/10.3389/fcvm.2022.933913>. Cited in: Pubmed; PMID 36003917.
- [34] Y. Xiao, Z. Teng, J. Xu, Q. Qi, T. Guan, X. Jiang, H. Chen, X. Xie, Y. Dong, P. Lv, Systemic immune-inflammation index is associated with cerebral small vessel disease burden and cognitive impairment, *eng. Epub* 2023/03/01, *Neuropsychiatric Dis. Treat.* 19 (2023) 403–413, <https://doi.org/10.2147/ndt.S401098>. Cited in: Pubmed; PMID 36852257.
- [35] T. Matsui, H. Arai, T. Yuzuriha, H. Yao, M. Miura, S. Hashimoto, S. Higuchi, S. Matsushita, M. Morikawa, A. Kato, H. Sasaki, Elevated plasma homocysteine levels and risk of silent brain infarction in elderly people, *eng. Epub* 2001/09/06, *Stroke* 32 (5) (2001 May) 1116–1119, <https://doi.org/10.1161/01.str.32.5.1116>. Cited in: Pubmed; PMID 11340219.
- [36] Y.L. Tseng, Y.Y. Chang, J.S. Liu, C.S. Su, S.L. Lai, M.Y. Lan, Association of plasma homocysteine concentration with cerebral white matter hyperintensity on magnetic resonance images in stroke patients, *eng. Epub* 2009/04/29, *J. Neurol. Sci.* 284 (1–2) (2009 Sep 15) 36–39, <https://doi.org/10.1016/j.jns.2009.03.030>. Cited in: Pubmed; PMID 19398115.

- [37] S. Seshadri, P.A. Wolf, A.S. Beiser, J. Selhub, R. Au, P.F. Jacques, M. Yoshita, I.H. Rosenberg, R.B. D'Agostino, C. DeCarli, Association of plasma total homocysteine levels with subclinical brain injury: cerebral volumes, white matter hyperintensity, and silent brain infarcts at volumetric magnetic resonance imaging in the Framingham Offspring Study, *eng. Epub 2008/05/14, Arch. Neurol.* 65 (5) (2008 May) 642–649, <https://doi.org/10.1001/archneur.65.5.642>. Cited in: Pubmed; PMID 18474741.
- [38] K.W. Nam, H.M. Kwon, H.Y. Jeong, J.H. Park, H. Kwon, S.M. Jeong, Serum homocysteine level is related to cerebral small vessel disease in a healthy population, *eng. Epub 2019/01/04, Neurology* 92 (4) (2019 Jan 22) e317–e325, <https://doi.org/10.1212/wnl.0000000000006816>. Cited in: Pubmed; PMID 30602466.
- [39] Y. Cao, N. Su, D. Zhang, L. Zhou, M. Yao, S. Zhang, L. Cui, Y. Zhu, J. Ni, Correlation between total homocysteine and cerebral small vessel disease: a Mendelian randomization study, *eng. Epub 2020/12/31, Eur. J. Neurol.* 28 (6) (2021 Jun) 1931–1938, <https://doi.org/10.1111/ene.14708>. Cited in: Pubmed; PMID 33377242.
- [40] R. Moretti, M. Giuffrè, P. Caruso, S. Gazzin, C. Tiribelli, Homocysteine in neurology: a possible contributing factor to small vessel disease, *Epub 2021/03/07, Int. J. Mol. Sci.* 22 (4) (2021 Feb 19) *eng.* <https://doi.org/10.3390/ijms22042051>. Cited in: Pubmed; PMID 33669577.
- [41] A. Hassan, B.J. Hunt, M. O'Sullivan, R. Bell, R. D'Souza, S. Jeffery, J.M. Bamford, H.S. Markus, Homocysteine is a risk factor for cerebral small vessel disease, acting via endothelial dysfunction, *eng. Epub 2003/11/11, Brain : J. Neurol.* 127 (Pt 1) (2004 Jan) 212–219, <https://doi.org/10.1093/brain/awh023>. Cited in: Pubmed; PMID 14607791.
- [42] P.K. Kamat, A. Kalani, S. Givvimani, P.B. Sathnur, S.C. Tyagi, N. Tyagi, Hydrogen sulfide attenuates neurodegeneration and neurovascular dysfunction induced by intracerebral-administered homocysteine in mice, *eng. Epub 2013/08/06, Neuroscience* 252 (2013 Nov 12) 302–319, <https://doi.org/10.1016/j.neuroscience.2013.07.051>. Cited in: Pubmed; PMID 23912038.